Published in final edited form as:
J Med Chem. 2009 August 13; 52(15): 4892–4902. doi:10.1021/jm900490a.

Design, Synthesis, and X-ray Crystal Structure of Classical and Nonclassical 2-Amino-4-oxo-5-substituted-6-ethyl-thieno[2,3-*d*] pyrimidines as Dual Thymidylate Synthase and Dihydrofolate Reductase Inhibitors and as Potential Antitumor Agents

Aleem Gangjee[*,†], **Wei Li**[†], **Roy L. Kisliuk**[‡], **Vivian Cody**[§], **Jim Pace**[§], **Jennifer Piriano**[§], and **Jennifer Makin**[§]

[†]Division of Medicinal Chemistry, Graduate School of Pharmaceutical Sciences, Duquesne University, 600 Forbes Avenue, Pittsburgh, PA 15282

[‡]Department of Biochemistry, School of Medicine, Tufts University, Boston, MA 02111

[§]Hauptman-Woodward Medical Research Institute, Inc., 700 Ellicott Street, Buffalo, New York 14203

Abstract

N-{4-[(2-amino-6-ethyl-4-oxo-3,4-dihydrothieno[2,3-*d*]pyrimidin-5-yl)thio]benzoyl}-L-glutamic acid **2** and thirteen nonclassical analogues **2a–2m** were synthesized as potential dual thymidylate synthase (TS) and dihydrofolate reductase (DHFR) inhibitors and as antitumor agents. The key intermediate in the synthesis was 2-amino-6-ethyl-5-iodothieno[2,3-*d*]pyrimidin-4(3*H*)-one, **7**, to which various aryl thiols were attached at the 5-position. Coupling **8** with L-glutamic acid diethyl ester and saponification afforded **2**. X-ray crystal structure of **2** and **1** (the 6-methyl analogue of **2**), DHFR and NADPH showed for the first time that the thieno[2,3-*d*]pyrimidine ring binds in a "folate" mode. Compound **2** was an excellent dual inhibitor of human TS (IC_{50} = 54 nM) and human DHFR (IC_{50} = 19 nM), and afforded nanomolar GI_{50} values against tumor cells in culture. The 6-ethyl substitution in **2** increases both the potency (by two- to three-orders of magnitude) as well as the spectrum of tumor inhibition in *vitro* compared to the 6-methyl analogue **1**. Some of the nonclassical analogues were potent and selective inhibitors of DHFR from *Toxoplasma gondii*.

Introduction

Folate metabolism has long been recognized as important and an attractive target for chemotherapy due to its crucial role in the biosynthesis of nucleic acid precursors.[1,2] Inhibitors of folate-dependent enzymes have found clinical utility as antitumor, antimicrobial, and antiprotozoal agents [2–5] (Figure 1). Thymidylate synthase (TS[a]), which catalyzes the reductive methylation of deoxyuridylate (dUMP) to thymidylate (dTMP), has been of particular interest.

*To whom correspondence should be addressed. Phone: 412-396-6070. Fax: 412-396-5593. E-mail: gangjee@duq.edu.

Supporting Information Available:
Results from elemental analysis and high resolution mass spectrometry. This material is available free of charge via the Internet at http://pubs.acs.org.

[a]Abbreviations: TS, thymidylate synthase; dUMP, deoxyuridylate; dTMP, deoxythymidylate; 7,8-DHF, 7,8-dihydrofolate; DHFR, dihydrofolate reductase; MTX, methotrexate; RFC, reduced folate carrier; FPGS, folylpolyglutamate synthetase; GARFT, glycinamide ribonucleotide formyltransferase; AICARFT, aminoimidazole carboxamide ribonucleotide formyltransferase; AIDS, acquired immunodeficiency syndrome; *P. carinii*, *Pneumocystis carinii*; *T. gondii*, *Toxoplasma gondii*; *E. coli*, *Escherichia coli*; PTX, piritrexim; NCI, National Cancer Institute.

[6,7] This reaction affords 7,8-dihydrofolate (7,8-DHF), which is reduced by dihydrofolate reductase (DHFR) to tetrahydrofolate (THF).[3, 5–7] Thus, TS and DHFR are crucial for the synthesis of dTMP in dividing cells. Several TS and DHFR inhibitors, as separate entities, have found clinical utility as antitumor agents.[8–12] Usually a 2,4-diamino-substituted pyrimidine ring is considered important for potent DHFR inhibitory activity, while a 2-amino-4-oxopyrimidine or 2-methyl-4-oxopyrimidine ring is considered important for potent TS inhibitory activity.[3,7,8] Examples of clinically used TS and DHFR inhibitors are raltitrexed,[12] pemetrexed[11] and methotrexate[13] (MTX) illustrated in Figure 1. Raltitrexed is a quinazoline analogue that is transported into cells via the reduced folate carrier (RFC) and undergoes rapid polyglutamylation by the enzyme folylpolyglutamate synthetase (FPGS). Raltitrexed is approved as a first-line agent for advanced colorectal cancer in several European countries, Australia, Canada, and Japan. In pemetrexed a pyrrole ring replaces the pyrazine of folic acid and a methylene group replaces the N10-nitrogen in the bridge.[11] Pemetrexed contains a 6-5 fused pyrrolo[2,3-*d*]pyrimidine scaffold and is designated a multitargeted antifolate (MTA). Pemetrexed and its polyglutamylated metabolites are reported to be inhibitors of several important folate-dependent enzymes including TS, DHFR, glycinamide ribonucleotide formyltransferase (GARFT), and aminoimidazole carboxamide ribonucleotide formyltransferase (AICARFT).[11,16,17]

As part of a continuing effort to develop novel classical antifolates as antitumor agents, Gangjee et al.[18] reported the synthesis of *N*-{4-[(2-amino-6-methyl-4-oxo-3,4-dihydrothieno[2,3-*d*]pyrimidin-5-yl)sulfanyl]benzoyl}-L-glutamic acid **1** (Figure 2) as a potent dual inhibitor of TS and DHFR with IC_{50} values in the 10^{-8} M range. Compound **1** also demonstrated moderate inhibitory activity against the growth of several human tumor cell lines in the National Cancer Institute (NCI)[19] preclinical *in vitro* screen, with GI_{50} values of 10^{-5} to 10^{-6} M or lower. The dual TS/DHFR inhibitory potency and tumor cell inhibitory activities of **1** were, in part, attributed to its C6-methyl group. Molecular modeling using SYBYL 8.0[20] indicated that compound **1** could bind to human DHFR in the "flipped" mode compared to folic acid, in which the sulfur atom of thieno ring is superimposed on to the 4-oxo moiety of folate. Additionally, molecular modeling of **1** in human TS also suggested that homologation of the C6-methyl to an ethyl could further enhance the hydrophobic interaction with Trp109 and perhaps the antitumor activity as well.

A disadvantage of classical antifolates as antitumor agents is that they require an active transport mechanism to enter cells, which, when impaired, causes tumor resistance.[21,22] In addition, cells that lack these transport mechanisms, including many bacterial and protozoan cells, are not susceptible to the action of classical antifolates.[23–26] In an attempt to overcome these potential drawbacks, nonclassical lipophilic antifolates have been developed as antitumor agents that do not require the folate transport system(s) but enter cells via diffusion. These lipophilic nonclassical antifolates such as nolatrexed (Figure 1) lack the polar glutamate moiety and hence do not depend on FPGS for their inhibitory activity.[27,28] In addition, nonclassical antifolates do not require the reduced folate carrier (RFC) system for active uptake into the cell since they are lipophilic and are passively transported into cells.

An additional aspect of our interest in nonclassical dual TS-DHFR inhibitors lies in the treatment of opportunistic infections in immunocompromised patients such as those with acquired immunodeficiency syndrome (AIDS).[29,30] The principal cause of death in patients with AIDS is opportunistic infections caused by *Pneumocystis carinii* (*P. carinii*)[31] and *Toxoplasma gondii* (*T. gondii*).[32] Current therapy includes the use of selective but weak inhibitors of protozoal DHFR such as trimethoprim (TMP) (Figure 1), in combination with sulfonamides to enhance potency. Toxicity of the sulfa drug component of these combinations is often a serious problem.[32] In addition, the potent but toxic nonclassical antifolates trimetrexate (TMQ) and piritrexim (PTX) (Figure 1), co-administered with leucovorin for host

rescue, are also used. Serious toxicities associated with the use of TMQ and PTX often force the cessation of treatment. Thus, it is of considerable interest to incorporate selectivity and potency into a single nonclassical antifolate that can be used alone to treat these infections.

Gangjee et al.[18] recently described the design and synthesis of several nonclassical 2-amino-4-oxo-5-arylthio-substituted-6-methylthieno[2,3-*d*]pyrimidine **1a–1i** (Figure 2) as dual TS/DHFR inhibitors. All of the nonclassical analogues were reasonably potent inhibitors of human TS with IC_{50} values ranging from 0.11 to 4.6 μM. The electronic nature of the substitutent on the side chain phenyl was an important factor in determining inhibitory potency. Analogues with electron withdrawing substitutions on the phenyl ring were more potent than analogues with electron donating substitutions or the unsubstituted phenyl. Structure activity relationship (SAR) studies demonstrated that analogues with electron withdrawing groups at the 3- and/or 4-positions of the phenyl side chain provided optimum inhibitory potency against human TS. Nonclassical analogues such as **1b** (IC_{50} = 0.26 μM), **1c** (IC_{50} = 0.11 μM), **1e** (IC_{50} = 0.11 μM), **1g** (IC_{50} = 0.12 μM) or **1h** (IC_{50} = 0.28 μM) were much more potent than the clinically used raltitrexed and pemetrexed against human TS, thus nonclassical analogues **2a–2m** containing similar phenyl substituents were also synthesized. Interestingly, all the nonclassical compounds **1a–1i**[18]were potent inhibitors of *T. gondii* DHFR with IC_{50} values ranging from 0.028 to 0.12 μM. The IC_{50} values of compounds **1b–1i** against *T. gondii* DHFR were similar in potency to MTX, and were about 243-fold more potent than the clinically used TMP. In addition, all the nonclassical compounds showed good to excellent selectivity against *T. gondii* DHFR as compared to human DHFR. Analogue **1c** (IC_{50} = 0.56 μM) was the most potent compound in this series against human DHFR, and it was 28-fold less potent against human DHFR than MTX but was more than 12-fold more potent than pemetrexed. Compound **1d** with a 2,5-dimethoxy substitution on the phenyl ring was marginally active against human DHFR (IC_{50} = 22 μM), but very potent against *T. gondii* DHFR (IC_{50} = 56 nM) exhibiting 393-fold selectivity compared to human DHFR. As indicated above, molecular modeling (SYBYL 8.0) suggested that an extension of the 6-methyl group to an ethyl group might enhance the potency and selectivity against some pathogenic TS and DHFR. To determine the effect of 6-ethyl homologation on human TS and DHFR inhibitory activity in the classical and nonclassical analogues, compounds **2-2m** (Figure 2) were synthesized. The synthesis and biological activities of analogues **2-2m** are the subject of this report.

Chemistry

The synthetic strategy for target compounds **2-2m** is shown in Scheme 1. The key intermediate in the synthesis was 2-amino-6-ethyl-5-iodothieno[2,3-*d*]pyrimidin-4(3*H*)-one, **6** (Scheme 1), which could undergo microwave assisted palladium catalyzed coupling reactions with appropriate aryl thiols to afford target compounds **2a–2m** and intermediate **7** for the synthesis of classical analogue **2**.

The required intermediate ethyl 2-amino-5-ethylthiophene-3-carboxylate, **4** was synthesized from commercially available butyraldehyde, **3** with ethylcyanoacetate, sulfur and triethylamine *via* reported methods of Gewald.[33] With compound **4** in hand, we turned our attention to its conversion to the 2-amino-6-ethylthieno[2,3-*d*]pyrimidin-4-(3*H*)-one, **5**. A literature search revealed that the synthesis of compound **5** was not reported. Gangjee et al.[34] had previously reported that chlorformamidine hydrochloride on cyclization with ethyl 2-amino-5-methylthiophene-3-carboxylate, gave 2-amino-6-methylthieno[2,3-*d*]pyrimidin-4(3*H*)-one in reasonably good yield. Thus heating a mixture of **4** and chlorformamidine hydrochloride in $DMSO_2$ under N_2 for a period of 2 h at 120–125 °C gave **5** in good yields (86%) after column chromatography.

Recently, we reported a convenient C5-bromination for the 2-amino-4-oxo-6-methyl-thieno [2,3-*d*]pyrimidine template with Br_2 under microwave irradiation.[18] To our surprise, all efforts to perform this halogenation of **5** with Br_2 or NBS using a variety of reaction conditions of time and temperature variations proved fruitless. Thus we had to consider an alternate halogenation method. A search of the literature revealed that there was no synthetic or other report for **6**. However, Taylor et al.[35] had reported mercuration methodology that could be adopted for the synthesis of the key intermediate 2-amino-6-ethyl-5-iodothieno[2,3-*d*] pyrimidin-4(3*H*)-one **6**. Extending this methodology to the synthesis of **6** required the 5-chloromercuri derivative, which was obtained by mercuration of **5** with mercurate acetate in glacial acetic acid at 100 °C for 3 h, followed by treatment with NaCl solution. Without separation, this 5-chloromercuri derivative was treated with iodoine in CH_2Cl_2 at room temperature for 5 h to afford **6** in 42% yield (over two steps). With the key intermediate **6** in hand, attention was turned to its conversion to the target compounds **2a–2m** and intermediate **7** (Scheme 1). Palladium-catalyzed cross-coupling reactions[36] to form carbon-sulfur bonds with aryl bromides and aryl thiols appeared attractive for the synthesis of the target compounds **2a–2m** and intermediate **7**. Initial attempts to react the iodo derivative **6** with corresponding aryl thiols catalyzed by $Pd_2(dba)_3$ with variations of time (up to 8 h) and temperature (up to reflux) were unsuccessful.

Failure of the above attempts led us to explore an alternative strategy to perform this palladium-catalyzed cross-coupling reaction. Microwave irradiation has been widely applied in organic synthesis resulting in faster and cleaner reactions that sometimes exhibit different reactivities due to specific microwave absorption. It was therefore of interest to attempt this cross-coupling reaction under microwave irradiation. Thus heating a mixture of **6**, the appropriate aryl thiols and *i*-Pr_2NEt in DMF in the presence of $Pd_2(dba)_3$ and Xantphos under microwave irradiation at 190 °C for 1 h afforded the corresponding target compounds **2a–2m** in the yields of 67–87%.

For the synthesis of the classical compound **2**, the required intermediate, methyl 4-[(2-amino-6-ethyl-4-oxo-3,4-dihydrothieno[2,3-*d*]pyrimidin-5-yl)thio]benzoate, **7** (Scheme 1), was prepared using the same synthetic strategy as shown for **2a–2m**. Methyl 4-mercaptobenzoate was used to afford **7** in a yield of 76%. Ester hydrolysis of **7** with 1 N NaOH at room temperature for 18 h afforded the corresponding free acid **8** in 96% yield. Coupling of the acid **8** (Scheme 1) with L-glutamic acid diethyl ester hydrochloride and 2-chloro-4,6-dimethoxy-l,3,5-triazine as the activating agent followed by column chromatographic purification afforded **9** in 70% yield. The ^1H NMR of **9** revealed the newly formed peptide NH proton at 8.61 ppm as a doublet, which exchanged on addition of D_2O. Compound **9** was characterized on the basis of NMR and MS. Hydrolysis of **9** with aqueous NaOH at room temperature, followed by acidification with 3 N HCl under ice cold conditions, afforded target compound **2** in 94% yield.

X-ray Crystal Structure

The X-ray crystal structures of the ternary complex of **2**, NADPH, and the human DHFR double mutants (Q35K/N64F and Q35S/N64S) were determined, as well as complexes of **1** with the Q35K single mutant protein and wild type human DHFR. All DHFR ternary complex structures were refined to 1.3-1.5 Å resolution. These results show, for the first time, that the thieno[2,3-*d*]pyrimidine antifolates **1** and **2** bind in a folate orientation such that the thieno sulfur occupies the N8 position observed in the binding of folic acid. Careful analysis of the difference electron density maps (Figure 3) was carried out to validate the binding orientation of **1** and **2**. The difference electron density for all structures reveals that the thieno ring of **1** and **2** bind in the folate orientation.

In these structures, the thieno ring has no hydrogen donor function. Nevertheless, the S7 of the thieno[2,3-*d*]pyrimidine ring makes intermolecular contacts with the carbonyl of Ile7 (3.6 Δ), Val115 (3.9 Δ), the hydroxyl of Tyr121 (3.8 Δ), and the carbonyl of the nicotinamide ring (3.4 Δ) (Figure 4). These values are longer than those observed for the 2,4-diamino pyrrolo[2,3-*d*] pyrimidine and furo[2,3-*d*]pyrimidine structures that showed a flipped orientation.[29,37,38]. Although molecular modeling studies carried out previously[18] predicted that both a flipped as well as folate binding orientation was possible for 2-amino-4-oxo-6-methyl thieno[2,3-d] pyrimidine, the structural data for four examples of **1** and **2** bound to mutant human DHFR all show binding in the folate orientation.

Biological Evaluation and Discussion

The classical analogue **2** and the nonclassical analogues **2a–2m** were evaluated as inhibitors of human, *Escherichia coli* (*E. coli*), and *T. gondii* DHFR[39] and TS.[40] The inhibitory potencies (IC_{50}) are listed in Table 1 and compared with pemetrexed, PDDF, MTX, and trimethoprim and the previously reported values for **1**.

The classical analogue **2** (Table 1) was an excellent dual inhibitor of human TS (IC_{50} = 54 nM) and human DHFR (IC_{50} = 19 nM). Against human TS, **2** was similar in potency to the previously reported compound **1** and about 2-fold more potent than PDDF and a remarkable 238-fold more potent than the clinically used pemetrexed.

Against human DHFR (Table 1) **2** was similar in potency to **1** and the clinically used MTX (Table 1) and was 330-fold more potent than pemetrexed. Interestingly, compound **2** was 9-fold more potent against *T. gondii* DHFR than human DHFR, indicating a significant species difference. Compound **2** was somewhat more potent than **1** as an inhibitor of human DHFR. This increase in activity against human DHFR of **2** over **1** may be attributed to increased hydrophobic interaction of the 6-ethyl moiety of **2** and Val115 in human DHFR as predicted from molecular modeling and confirmed by the X-ray crystal structure (Figure 6). The biological data (IC_{50}) of compounds **1** and **2** indicate that the methyl and ethyl groups at the C6-position respectively are both conducive for potent human TS and DHFR inhibition.

The nonclassical analogues **2a–2m** were also evaluated as inhibitors of TS and DHFR (Table 1). In the human TS assay, all of the nonclassical analogues were reasonably potent inhibitors with IC_{50} values ranging from 0.22 to 5.6 μM. The electronic nature of the substitutent on the side chain phenyl was an important factor in determining inhibitory potency. Analogues with electron withdrawing substitutions on the phenyl ring were more potent than analogues with electron donating substitutions or the unsubstituted phenyl. Electron withdrawing, 4-nitro, 3,4-dichloro, 3-chloro and 4-bromo substituents in analogues **2c**, **2e**, **2k** and **2j**, respectively, showed the most potent inhibition against isolated human TS. In addition, bulky substituents such as the 2-naphthyl (**2g**) showed marginal activity against human TS. These data are consistent with SAR studies previously reported for the C6-methyl analogues.[18] The nonclassical analogues **1b**, **1c**, **1e**, **1g** and **1h** of the 6-methyl series were potent human TS inhibitors.[18] The corresponding 6-ethyl analogues **2b**, **2c**, **2e**, **2g** and **2h** of this study were similar in potency except for **2g** which was about 20-fold less potent than **1g**. This difference in potency may reflect a steric intolerance of the larger 6-ethyl moiety with an adjacent naphthyl ring in **2g**. Similar to the classical analogue **2**, all of the nonclassical analogues were also more potent than pemetrexed as inhibitors of human TS. This result indicates that homologation of a 6-methyl to a 6-ethyl in thieno[2,3-*d*]pyrimidines maintains potent human TS inhibitory activity.

In the DHFR assay, the nonclassical analogues **2a–2m** were also evaluated as inhibitors of human, *E. coli* and *T. gondii* DHFR. Against human DHFR, in general **2a–2m** were moderately

potent inhibitors with IC_{50} values ranging from 0.26 to 2.2 μM, and were more potent than the corresponding 6-methyl analogues.[18] The most potent nonclassical analogues contained electron withdrawing groups such as 4-nitrophenyl **2c** (IC_{50} = 0.26 μM) and 4-bromophenyl **2j** (IC_{50} = 0.26 μM) in the 6-ethyl (**2a–2m**) series. Other substitutions such as an unsubstituted phenyl **2a** (IC_{50} = 2.6 μM) and unsubstituted 2-naphthyl **2g** (IC_{50} = 2.2 μM) cause a 10-fold drop in activity. In addition, compound **2c** was the most potent compound in the nonclassical series, also demonstrating potent dual inhibitory activities against human TS (IC_{50} = 0.22 μM) and human DHFR (IC_{50} = 0.26 μM). The SAR among these analogues (**2a–2m**) suggests that potency for human DHFR is independent of the electronic nature of the substituent but mono para-electron withdrawing substitution is most favorable for human DHFR inhibition. Against *T. gondii* DHFR, in general, the nonclassical analogues **2a–2m** were very potent inhibitors with IC_{50} values ranging from 0.27 to 0.0081 μM. The most potent single digit nanomolar nonclassical inhibitors contained electron withdrawing groups such as a 4-chlorophenyl **2b** (IC_{50} = 0.009 μM), 4-nitrophenyl **2c** (IC_{50} = 0.0087 μM), 3,4-dichlorophenyl **2e** (IC_{50} = 0.0081 μM) and 2-naphthyl **2g** (IC_{50} = 0.0084 μM). The IC_{50} values of compounds **2b**, **2c**, **2e** and **2g** against *T. gondii* DHFR were a remarkable 4-fold more potent than MTX, and were about 840-fold more potent than the clinically used trimethoprim (Table 1). To our knowledge these are some of the most potent nonclassical *T. gondii* DHFR inhibitors reported. Interestingly, a number of the nonclassical compounds in this series also showed good selectivity for *T. gondii* DHFR as compared to human DHFR. Compound **2g** with a 2-naphthyl substitution was 262-fold more selective for *T. gondii* DHFR than human DHFR, which indicated a distinct species difference in DHFR from different sources. These results demonstrate that the nonclassical analogues **2a–2m** in the 6-ethyl series follow similar trends of dual inhibition against human TS and DHFR as the 6-methyl analogues.

The classical analogue **2** was selected by the National Cancer Institute (NCI) for evaluation in its in vitro preclinical antitumor screening program. The full NCI panel of approximately 60 human cancer cell lines are grouped into disease subpanels including leukemia, nonsmall-cell lung, colon, central nervous system (CNS), melanoma, ovarian, renal, prostate, and breast tumors cell lines. The ability of compound **2** to inhibit the growth of tumor cell lines was measured as GI_{50} values, the concentration required to inhibit the growth of tumor cells in culture by 50% as compared to a control. In 8 of the 60 cell lines, compound **2** showed GI_{50} values of $< 10^{-6}$ M (Table 2). It was also interesting to note that compound **2** was not a general cell poison but showed selectivity both within a type of tumor cell line as well as across different tumor cell lines with inhibitory values that in some instances differed by 1000-fold (data not shown). In addition, potency of tumor inhibition (GI_{50}) was significantly increased for **2** over **1** (Table 2) by a hundred- to thousand-fold, indicating that homologation of the 6-methyl to the 6-ethyl was instrumental in increasing the potency as well as the spectrum of tumor inhibition in culture (Table 2). Thus the in vitro tumor cell inhibitory activity of **2** was much superior to that of **1**. Possible explanation for this increased *in vivo* activity could be the increased lipophilicity of **2** compared to **1**, which could facilitate passive diffusion and/or active transport of **2** into tumor cells. This is currently under investigation. Compound **2** is also currently under further evaluation by the NCI as an antitumor agent.

In summary, the 5-substituted 2-amino-4-oxo-6-ethyl-thieno[2,3-*d*]pyrimidine classical antifolate **2** and thirteen nonclassical analogues **2a–2m** were designed and synthesized as potential dual TS-DHFR inhibitor. Compound **2** (TS IC_{50}= 54 nM; DHFR IC_{50}= 19 nM) maintained the potent human TS and DHFR inhibitory activity of **1**. More importantly compound **2** significantly increased both the spectrum as well as the potency of the inhibition of the growth of tumor cells in culture compared with **1**. This increase was clearly not attributable to enzyme inhibition difference because both **1** and **2** have about the same activity in isolated enzyme assays. Compound **2c** was the most potent compound in the nonclassical series, also demonstrating potent dual inhibitory activities against human TS (IC_{50} = 0.22 μM)

and human DHFR (IC_{50} = 0.26 μM). In addition, excellent potency and high selectivity for *T. gondii* DHFR compared to human DHFR was observed for all the analogues. This study indicated that the 5-substituted 2-amino-4-oxo-6-ethyl-thieno[2,3-*d*]pyrimidine scaffold is most conducive to dual human TS-DHFR inhibitory activity. The most remarkable finding was that elongation of the C6-methyl moiety of 2-amino-4-oxo-5-arylthio-substituted thieno[2,3-*d*]pyrimidine **1** to the 6-ethyl in **2** increases the inhibitory potency against the growth of several tumor cells in culture by two to three orders of magnitude and also increases the spectrum of tumor growth inhibition. These results are currently under investigation and may reflect transport and/or other differences between **1** and **2**.

Experimental Section

Analytical samples were dried in vacuo (0.2 mm Hg) in a CHEM-DRY drying apparatus over P_2O_5 at 80 °C. Melting points were determined on a MEL-TEMP II melting point apparatus with FLUKE 51 K/J electronic thermometer and are uncorrected. Nuclear magnetic resonance spectra for proton (^{1}H NMR) were recorded on a Bruker WH-400 (400 MHz) spectrometer. The chemical shift values are expressed in ppm (parts per million) relative to tetramethylsilane as an internal standard: s, singlet; d, doublet; t, triplet; q, quartet; m, multiplet; br, broad singlet. Mass spectra were recorded on a VG-7070 double-focusing mass spectrometer or in a LKB-9000 instrument in the electron ionization (EI) mode. Chemical names follow IUPAC nomenclature. Thin-layer chromatography (TLC) was performed on Whatman Sil G/UV254 silica gel plates with a fluorescent indicator, and the spots were visualized under 254 and 366 nm illumination. Proportions of solvents used for TLC are by volume. Column chromatography was performed on a 230–400 mesh silica gel (Fisher, Somerville, NJ) column. Elemental analyses were performed by Atlantic Microlab, Inc., Norcross, GA. Element compositions are within 0.4% of the calculated values. Fractional moles of water or organic solvents frequently found in some analytical samples of antifolates could not be prevented in spite of 24–48 h of drying in vacuo and were confirmed where possible by their presence in the ^{1}H NMR spectra. Microwave-assisted synthesis was performed utilizing an Emrys Liberator microwave synthesizer (Biotage) utilizing capped reaction vials. All microwave reactions were performed with temperature control. All solvents and chemicals were purchased from Aldrich Chemical Co. or Fisher Scientific and were used as received.

Ethyl 2-amino-5-ethylthiophene-3-carboxylate (4)

Et_3N (4.7 g, 0.05 mol) was added to a stirred suspension of ethylcyanoacetate (9.74 g, 90 mmol) and sulfur (2.76 g, 90 mol) in 50 mL DMF under a N_2 atmosphere. The resulting mixture was stirred at 55 °C (temperature of bath) for 1 h. Butyraldehyde **3** (6.5 g, 90 mmol) was then added into this suspension dropwise while maintaining the temperature at 55° C. After addition, the reaction was allowed to cool to room temperature and stirred for 2 h. The mixture was transferred to a separating funnel containing ethyl acetate (80 mL) and H_2O (30 mL). The organic layer was separated, washed with brine (4 × 20 mL), and concentrated under reduced pressure to afford yellow oil. The residue was loaded on a column packed with silica gel and eluted with 5% ethyl acetate in hexanes and fractions containing the desired product (TLC) were pooled and evaporated to afford 8.9 g (56%) of **4** as a yellow solid: mp 70–72° C; R_f 0.45 (ethyl acetate/n-hexane, 1:3); ^{1}H NMR (DMSO-d_6) δ 1.08 (t, 3 H, *J* = 7.2 Hz), 1.19 (t, 3 H, *J* = 7.2 Hz), 2.48 (q, 2 H, *J* = 7.2 Hz), 4.11 (q, 2 H, *J* = 7.2 Hz), 6.45 (s, 1H), 7.07 (s, 2 H).

2-Amino-6-ethylthieno[2,3-*d*]pyrimidin-4-(3*H*)-one (5)

Ethyl 2-amino-5-ethylthiophene-3-carboxylate **4** (9.5 g, 47.8 mmol), carbamimidic chloride hydrochloride (5.5 g, 48.3 mmol) and 25 g $DMSO_2$ was placed in a 250 mL flask. The reaction mixture was heated to 120–125 °C under N_2 for 2 h. Then H_2O (50 mL) was added to the reaction mixture right away to quench the reaction. The resulting solution was cooled in an ice

bath, and the pH was adjusted to 8 with dropwise addition of concentrated NH_4OH with stirring. This suspension was left at 5° C for 3 h and filtered. The residue was washed well with small amounts of acetone and water, purified by flash chromatography on silica gel (gradient: 2% MeOH/$CHCl_3$ to 5% MeOH/$CHCl_3$) to afford 8.1 g (86%) of **5** as a yellow solid: mp 126–128° C; R_f 0.63 (MeOH/$CHCl_3$, 1:10); ^{1}H NMR (DMSO-d_6) δ 1.20 (t, 3 H, J = 7.6 Hz), 2.71 (q, 2 H, J = 7.6 Hz), 6.45 (s, 2 H), 6.79 (s, 1 H), 10.82 (s, 1 H). Anal. ($C_8H_9N_3OS$•0.09CH_3COCH_3) C, H, N, S.

2-Amino-6-ethyl-5-iodothieno[2,3-*d*]pyrimidin-4(3*H*)-one (6)

To a suspension of **5** (3.5 g, 17.9 mmol) in 50 mL of glacial acetic acid at room temperature was added mercuric acetate (8.5 g, 26.8 mmol). The resulting solution was stirred at 100 °C for 3 h, then poured into a saturated NaCl (50 mL), and stirred for 20 min. The solid was collected by filtration, washed with water (20 mL), hexane (20 mL) and dried to give a dark solid (5-chloromercury derivative), which was directly used for iodination reaction without further purification. This dark material was dissolved in CH_2Cl_2 (30 mL) containing I_2 (6.8 g, 26.8 mmol), stirred for 5 h at room temperature. The solvent was evaporated, the residue was washed with 2 N NaS_2O_3 (35 mL) and dried in vacuo. The crude product was purified by column chromatography on silica gel with 3% MeOH/$CHCl_3$ as the eluent to afford 2.4 g (42%) of **6** as a white solid: mp 185–187° C; R_f 0.45 (MeOH/$CHCl_3$, 1:5); ^{1}H NMR (DMSO-d_6) δ 1.13 (t, 3 H, J = 7.6 Hz), 2.67 (q, 2 H, J = 7.6 Hz), 6.57 (s, 2 H), 10.93 (s, 1 H). Anal. ($C_8H_8IN_3OS$•0.34CH_2Cl_2) C, H, N, I, S.

Methyl 4-[(2-amino-6-ethyl-4-oxo-3,4-dihydrothieno[2,3-*d*]pyrimidin-5-yl)thio]benzoate (7)

The microwave reaction vial was charged with **6** (1.05 g, 3.3 mmol), *i*-Pr_2NEt (1.2 mL, 6.6 mmol) and 15 mL dry DMF. The mixture was evacuated and backfilled with nitrogen (3 cycles). Catalyst Pd_2dba_3 (76 mg, 0.08 mmol), Xantphos (94 mg, 0.16 mmol) and methyl 4-mercaptobenzoate (1.1 g, 6.6 mmol) were added and then the reaction mixture was degassed twice. The reaction mixture was irradiated in a microwave apparatus at 190° C, 1 h. After the reaction mixture was cooled to ambient temperature, the product was filtered, the filtrate was concentrated, and the crude mixture was purified by silica gel column chromatography using 2% MeOH in $CHCl_3$ as the eluent. Fractions containing the product (TLC) were combined and evaporated to afford 0.9 g (76%) of **7** as a white solid: R_f = 0.47 (MeOH/$CHCl_3$, 1:5); mp 156–158° C; ^{1}H NMR (DMSO-d_6) δ 1.10 (t, 3 H, J = 7.2 Hz), 2.81 (q, 2 H, J = 7.2 Hz), 6.61 (s, 2 H), 7.05 (d, 2 H, J = 8.4 Hz), 7.77 (d, 2 H, J = 8.4 Hz), 10.79 (s, 1 H). HRMS (EI) calcd for $C_{16}H_{15}N_3O_3S_2$ *m/z* = 361.0554, found *m/z* = 361.0556.

2-Amino-6-ethyl-5-(phenylsulfanyl)thieno[2,3-*d*]pyrimidin-4(3*H*)-one (2a)

Compound **2a** (synthesized as described for **7**): yield 87%; mp 215–220° C; TLC R_f = 0.48 ($CHCl_3$/MeOH, 5:1); ^{1}H NMR (DMSO-d_6) δ 1.10 (t, 3 H, J = 7.6 Hz), 2.82 (q, 2 H, J = 7.6 Hz), 6.57 (s, 2 H), 6.97–7.24 (m, 5 H), 10.76 (s, 1 H). HRMS (EI) calcd for $C_{14}H_{13}N_3OS_2$ *m/z* = 303.0500, found *m/z* = 303.0503.

2-Amino-5-[(4-chlorophenyl)sulfanyl]-6-ethylthieno[2,3-*d*]pyrimidin-4(3*H*)-one (2b)

Compound **2b** (synthesized as described for **7**): yield 81%; mp 174–175° C; TLC R_f = 0.47 ($CHCl_3$/MeOH, 5:1); ^{1}H NMR (DMSO-d_6) δ 1.11 (t, 3 H, J = 7.6 Hz), 2.82 (q, 2 H, J = 7.6 Hz), 6.59 (s, 2 H), 6.98 (d, 2 H, J = 8.4 Hz), 7.27 (d, 2 H, J = 8.4 Hz), 10.76 (s, 1 H). HRMS (EI) calcd for $C_{14}H_{12}N_3OClS_2$ *m/z* = 337.0110, found *m/z* = 337.0093.

2-Amino-6-ethyl-5-[(4-nitrophenyl)sulfanyl]thieno[2,3-*d*]pyrimidin-4(3*H*)-one (2c)

Compound **2c** (synthesized as described for **7**): yield 74%; mp 162–163° C; TLC R_f = 0.48 ($CHCl_3$/MeOH, 5:1); ^{1}H NMR (DMSO-d_6) δ 1.12 (t, 3 H, J = 7.6 Hz), 2.82 (q, 2 H, J = 7.6

Hz), 6.64 (s, 2 H), 7.16 (d, 2 H, *J* = 9.2 Hz), 8.07 (d, 2 H, *J* = 9.2 Hz), 10.83 (s, 1 H). HRMS (EI) calcd for $C_{14}H_{13}N_4O_3S_2$ *m/z* = 349.0429, found *m/z* = 349.0403.

2-Amino-5-[(2,5-dimethoxyphenyl)sulfanyl]-6-ethylthieno[2,3-*d*]pyrimidin-4(3*H*)-one (2d)

Compound **2d** (synthesized as described for **7**): yield 82%; mp 178–180° C; TLC R_f = 0.50 ($CHCl_3$/MeOH, 5:1); ^{1}H NMR (DMSO-*d6*) δ 1.08 (t, 3 H, *J* = 7.2 Hz), 2.77 (q, 2 H, *J* = 7.2 Hz), 3.52 (s, 3 H), 3.79 (s, 3 H), 5.92 (s, 2 H), 6.58–6.88 (m, 3 H), 10.78 (s, 1 H). HRMS (EI) calcd for $C_{16}H_{17}N_3O_3S_2$ *m/z* = 363.0711, found *m/z* = 363.0706.

2-Amino-5-[(3,4-dichlorophenyl)thio]-6-ethylthieno[2,3-*d*]pyrimidin-4(3*H*)-one (2e)

Compound **2e** (synthesized as described for **7**): yield 72%; mp 154-116° C; TLC R_f = 0.48 ($CHCl_3$/MeOH, 5:1); ^{1}H NMR (DMSO-d_6) δ 1.12 (t, 3 H, *J* = 7.6 Hz), 2.86 (q, 2 H, *J* = 7.6 Hz), 6.62 (s, 2 H), 6.90 (dd, 1 H, *J* = 2.4 Hz, *J* = 8.4 Hz), 7.3 (d, 2 H, *J* = 2.4 Hz), 7.46 (d, 1 H, *J* = 8.4 Hz), 10.80 (s, 1 H). HRMS (EI) calcd for $C_{14}H_{11}N_3OS_2Cl_2$ *m/z* = 370.9715, found *m/z* = 370.9720.

2-Amino-5-[(3,5-dichlorophenyl)sulfanyl]-6-ethylthieno[2,3-*d*]pyrimidin-4(3*H*)-one (2f)

Compound **2f** (synthesized as described for **7**): yield 74%; mp 176–178° C; TLC R_f = 0.45 ($CHCl_3$/MeOH, 5:1); ^{1}H NMR (DMSO-d_6) δ 1.12 (t, 3 H, *J* = 7.6 Hz), 2.84 (q, 2 H, *J* = 7.6 Hz), 6.58 (s, 2 H), 6.98 (s, 1 H), 7.05 (s, 1 H), 7.20 (s, 1 H), 10.76 (s, 1 H). HRMS (EI) calcd for $C_{14}H_{11}N_3OS_2Cl_2$ *m/z* = 370.9708, found *m/z* = 370.9720.

2-Amino-6-ethyl-5-(2-naphthylthio)thieno[2,3-*d*]pyrimidin-4(3*H*)-one (2g)

Compound **2g** (synthesized as described for **7**): yield 87%; mp 154–156° C; TLC R_f = 0.51 ($CHCl_3$/MeOH, 5:1); ^{1}H NMR (DMSO-d_6) δ 1.12 (t, 3 H, *J* = 7.2 Hz), 2.86 (q, 2 H, *J* = 7.2 Hz), 6.59 (s, 2 H), 7.15–7.82 (m, 7 H), 10.74 (s, 1 H). HRMS (EI) calcd for $C_{18}H_{15}N_3OS_2$ *m/z* = 353.0656, found *m/z* = 353.0653.

2-Amino-6-ethyl-5-(pyridin-4-ylsulfanyl)thieno[2,3-*d*]pyrimidin-4(3*H*)-one (2h)

Compound **2h** (synthesized as described for **7**): yield 67%; mp 185–186° C; TLC R_f = 0.50 ($CHCl_3$/MeOH, 5:1); ^{1}H NMR (DMSO-d_6) δ 1.11 (t, 3 H, *J* = 7.2 Hz), 2.80 (q, 2 H, *J* = 7.2 Hz), 6.63 (s, 2 H), 6.92 (d, 2 H, J = 4.8 Hz), 8.28 (d, 2 H, J = 4.8 Hz), 10.83 (s, 1 H). HRMS (EI) calcd for $C_{13}H_{13}N_4OS_2$ *m/z* = 305.0531, found *m/z* = 305.0528.

2-Amino-6-ethyl-5-[(4-fluorophenyl)sulfanyl]thieno[2,3-d]pyrimidin-4(3*H*)-one (2i)

Compound **2i** (synthesized as described for **7**): yield 75%; mp 194–196° C; TLC R_f = 0.50 ($CHCl_3$/MeOH, 5:1); ^{1}H NMR (DMSO-d_6) δ 1.12 (t, 3 H, *J* = 7.2 Hz), 2.84 (q, 2 H, *J* = 7.2 Hz), 6.59 (s, 2 H), 7.07–7.09 (m, 4 H), 10.77 (s, 1 H). HRMS (EI) calcd for $C_{14}H_{12}N_3OFS_2$ *m/z* = 321.0405, found *m/z* = 321.0404.

2-Amino-5-[(4-bromophenyl)sulfanyl]-6-ethylthieno[2,3-*d*]pyrimidin-4(3*H*)-one (2j)

Compound **2j** (synthesized as described for **7**): yield 74%; mp 186–187° C; TLC R_f = 0.51 ($CHCl_3$/MeOH, 5:1); ^{1}H NMR (DMSO-*d6*) δ 1.11 (t, 3 H, *J* = 7.2 Hz), 2.82 (q, 2 H, *J* = 7.2 Hz), 6.60 (s, 2 H), 6.92 (d, 2 H, *J* = 6.8 Hz), 7.39 (d, 2 H, *J* = 6.8 Hz), 10.76 (s, 1 H). HRMS (EI) calcd for $C_{14}H_{12}N_3OBrS_2$ *m/z* = 380.9611, found *m/z* = 380.9605.

2-Amino-5-[(3-chlorophenyl)sulfanyl]-6-ethylthieno[2,3-*d*]pyrimidin-4(3*H*)-one (2k)

Compound **2k** (synthesized as described for **7**): yield 72%; mp 186–187° C; TLC R_f = 0.53 ($CHCl_3$/MeOH, 5:1); ^{1}H NMR (DMSO-d_6) δ 1.14 (t, 3 H, *J* = 7.2 Hz), 2.87 (q, 2 H, *J* = 7.2

Hz), 6.62 (s, 2 H), 6.90 (m, 3 H), 7.24 (s, 1H), 10.80 (s, 1 H). HRMS (EI) calcd for $C_{14}H_{12}ClN_3OS_2$ *m/z* = 337.0119, found *m/z* = 337.0110.

2-Amino-5-[(3,5-dimethoxyphenyl)sulfanyl]-6-ethylthieno[2,3-*d*]pyrimidin-4(3*H*)-one (2l)

Compound **2l** (synthesized as described for **7**): yield 83%; mp 151–154° C; TLC R_f = 0.45 ($CHCl_3$/MeOH, 5:1); ^{1}H NMR (DMSO-d_6) δ 1.14 (t, 3 H, *J* = 7.6 Hz), 2.89 (q, 2 H, *J* = 7.6 Hz), 3.67 (s, 3 H), 6.55 (s, 2 H), 6.56 (dd, 1 H, *J* = 2.4 Hz, *J* = 8.4 Hz), 6.83 (d, 2 H, *J* = 2.4 Hz), 6.87 (d, 1 H, *J* = 8.4 Hz), 10.78 (s, 1 H). HRMS (EI) calcd for $C_{16}H_{17}N_3O_3S_2$ *m/z* = 363.0721, found *m/z* = 363.0711.

2-Amino-5-[(2-chlorophenyl)sulfanyl]-6-ethylthieno[2,3-*d*]pyrimidin-4(3*H*)-one (2m)

Compound **2m** (synthesized as described for **7**): yield 72%; mp 221–224° C; TLC R_f = 0.53 ($CHCl_3$/MeOH, 5:1); ^{1}H NMR (DMSO-d_6) δ 1.14 (t, 3 H, *J* = 7.2 Hz), 2.85 (q, 2 H, *J* = 7.2 Hz), 6.63 (s, 2 H), 6.90 (m, 4 H), 10.80 (s, 1 H). HRMS (EI) calcd for $C_{14}H_{12}ClN_3OS_2$ *m/z* = 337.0113, found *m/z* = 337.0110.

4-[(2-Amino-6-ethyl-4-oxo-3,4-dihydrothieno[2,3-*d*]pyrimidin-5-yl)thio]benzoic acid (8)

To a solution of **7** (0.72 g, 1.6 mmol) in MeOH (10 mL) was added 1 N NaOH (32 mL) and the reaction mixture stirred at room temperature for 18 h until TLC showed that the reaction was complete. The reaction mixture was evaporated to dryness under reduced pressure. The residue was dilute with H_2O (5 mL). The resulting solution was adjusted to pH 4 with 3 N aq HCl then stored at 0° C for 24 h. The precipitated solid was collected and dried in vacuo using P_2O_5 to afford 0.53 g (96%) of **8** as a white powder: mp 216–218° C; R_f 0.34 (MeOH/$CHCl_3$, 1:4); ^{1}H NMR (DMSO-d_6) δ 1.13 (t, 3 H, *J* = 7.6 Hz), 2.83 (q, 2 H, *J* = 7.6 Hz), 6.62 (s, 2 H), 7.03 (d, 2 H, *J* = 8.4 Hz), 7.76 (d, 2 H, *J* = 8.4 Hz), 10.79 (s, 1 H). Anal. (C15H13N3O3S2•1.94CH_3COCH_3) C, H, N, S.

Diethyl *N*-{4-[(2-amino-6-ethyl-4-oxo-3,4-dihydrothieno[2,3-*d*]pyrimidin-5-yl)thio]-benzoyl}-L-glutamate (9)

To a suspension of benzoic acid **8** (0.4 g, 1.1 mmol) in DMF (10 mL) at 25 °C was added *N*-methylmorpholine (0.12 mL, 1.21 mmol) followed by 2-chloro-4,6-dimethoxy-1,3,5-triazine (0.21 g, 1.1 mmol), and the resulting solution was stirred at 25° C for 2 h. At this point, *N*-methylmorpholine (0.12 mL, 1.21 mmol) was added to this solution followed by L-glutamic acid diethyl ester hydrochloride (0.31 g, 1.32 mmol), and the resulting mixture was stirred at 25° C for another 4 h until the starting material **8** disappeared (TLC). The reaction solution was evaporated in vacuo to dryness, and the residue was purified by column chromatography on silica gel with 5% MeOH in $CHCl_3$ as the eluent. Fractions containing the product (TLC) were combined and evaporated to afford 0.41 g (70%) of **9** as a white solid: mp 150–152° C; R_f 0.57 (MeOH/$CHCl_3$, 1:5); ^{1}H NMR (DMSO-d_6) δ 1.12–1.17 (m, 6 H), 1.14 (t, 3 H, *J* = 7.6 Hz), 1.93–2.10 (m, 2 H), 2.39 (m, 2 H), 2.86 (q, 2 H, *J* = 7.6 Hz), 4.05 (m, 4 H), 4.37 (m, 1 H), 6.61 (s, 1 H), 7.02 (d, 2 H, *J* = 8.4 Hz), 7.69 (d, 2 H, *J* = 8.4 Hz), 8.61 (d, 1 H, *J* = 7.6 Hz), 10.79 (br s, 1 H). Anal. ($C_{24}H_{28}N_4O_6S_2$·0.59CH_3COCH_3) C, H, N, S. HRMS (EI) calcd for $C_{24}H_{28}N_4O_6S_2$ *m/z* = 532.1450, found *m/z* = 532.1444.

N-{4-[(2-amino-6-ethyl-4-oxo-3,4-dihydrothieno[2,3-*d*]pyrimidin-5-yl)thio]benzoyl }-L-glutamic acid (2)

To a solution of **9** (0.35 g, 0.65 mmol) in ethanol (10 mL) was added 1 N NaOH (10 mL), and the mixture was stirred at room temperature for 24 h until the starting material **9** disappeared (TLC). The reaction mixture was evaporated to dryness under reduced pressure. The residue was dissolved in water (3 mL), the resulting solution was cooled in an ice bath, and the pH was adjusted to 3–4 with dropwise addition of 3 N HCl. This suspension was left at 5° C for 24 h.

The precipitated solid was collected by filtration, washed with brine, and dried in vacuo to afford **3** (0.31 g, 94%) of as an offwhite solid: mp 202–204° C; R_f 0.35 (MeOH/$CHCl_3$, 1:4); 6.61 (s, 1 H), 7.02 (d, 2 H, *J* = 8.0 Hz), 7.69 (d, 2 H, *J* = 8.0 Hz), 8.61 (d, 1 H, *J* = 7.6 Hz), 10.79 (br s, 1 H). Anal. ($C_{20}H_{20}N_4O_6S_2$•0.31CH_3COCH_3 . 0.79HCl) C, H, N, S.

Construction and Expression of Mutant Human DHFR

Mutations were introduced into the cDNA of human DHFR and verified by sequencing (Roswell Park Cancer Center, Buffalo, NY). DNA oligonucleotides were obtained from Integrated DNA Technologies (Coralville, IA) and used without further purification.

mutants in pDS5

Plasmid DNA was purified using the plasmid mini kit (Qiagen). Mutagenesis was performed using the QuikChange Site-Directed Mutagenesis Kit (Stratagene). All primers were PAGE purified and were synthesized by Alpha DNA (Montreal, Quebec) or IDT (Coralville, IA). Primers were designed according to manufacturer's recommendations. PCR reactions were performed according to manufacturer's recommendations with adjustments made for T_m of corresponding primers.

Primers (5' to 3')

N65F for:	GGTTCTCCATTCCTGAGAAGTTTCGACCTTTAAAGGGTAG
N65F rev:	CTACCCTTTAAAGGTCGAAACTTCTCAGGAATGGAGAACC
N65S for:	GGTTCTCCATTCCTGAGAAGAGTCGACCTTTAAAGGGTAG
N65S rev:	CTACCCTTTAAAGGTCGACTCTTCTCAGGAATGGAGAACC
Q36K for:	CAGATATTTCAAGAGAATGACCACAACC
Q36K rev:	GGTTGTGGTCATTCTCTTGAAATATCTG
Q36S for:	CAGATATTTCTCGAGAATGACCACAACC
Q36S rev:	GGTTGTGGTCATTCTCGAGAAATATCTG

The original wt human DHFR (pDS5 vector) was used for PCR and all subsequent mutagenesis experiments. Four single mutants were created (N65F, N65S, Q36K, Q36S) with the QuikChange Site Directed Mutagenesis Kit following the manufacturer's recommended conditions.

PCR: (50ng of dsDNA template, 100ng of each primer, 5mM dNTPs, 2.5U/μL Taq) 1 cycle of 95EC for 30sec, 16 cycles of 95EC for 30sec, 55EC for 1min, 68EC for 3min The two double mutants (Q35K/N64F and Q35S/N64S) were created by using parental template DNA having one confirmed single residue mutation and using primers for the second desired mutation during PCR.

Expression and purification of human DHFR pDS5/mutant pDS5

Expression of mutant human DHFR in pDS5 vector in *E. coli* BL21 (DE3) carried out with 200 mL of LB medium containing 100 ug/mL ampicillin and inoculated with glycerol stock of human DHFR at 37EC with shaking at 300 rpm overnight. One liter of fresh LB/AMP was inoculated with the 200 mL overnight culture. The culture was grown at 37E C at 300 rpm until the $O.D._{600}$ 0.8–0.9. Cells were then induced with 2 mM IPTG overnight at 16E C (16–18 hr) and harvested by centrifugation at 13,000 × g. Cells were resuspended in 100 mL of ice-cold M9 salt solution (12.8 g Na_2HPO4-$7H_20$, 3 g KH_2PO_4, 0.5 g NaCl, 1 g NH_4Cl in a volume of 1 L).

Cells were lysed in 100 mL of ice-cold buffer containing 6.8 g KH_2PO_4, 3.7 g KCl, dissolved in 900 mL of H_20, 1.0 mL of 1.0 M EDTA is added and the pH adjusted to 7.0 with KOH before bringing volume to 1 L. Cells were disrupted by passing through a microfluidizer at 18,000 psi (Microfluidics, Inc). The resulting lysate was subjected to centrifugation for 30 min. at 7,000 × g. Ammonium sulfate was added to supernatant over a period of 60 min. to a final saturation of 85% at 0E C. Precipitated protein was centrifuged for 30 min. at 7,000 × g and the pellet resuspended in 50 mL of methotrexate column binding buffer (100 mM KCl, 50 mM KPO_4, pH 7.0). The resulting sample was passed over a 25 mL methotrexate affinity column. The column was extensively washed (> 5 column volumes of buffer) to remove unbound protein. DHFR was subsequently eluted in 5 mL fractions by passing a solution of 4 mM folic acid, 50 mM KPO_4, pH 8.0 over the column. SDS-PAGE was performed on fractions to determine which contain DHFR. The corresponding fractions were then pooled and dialyzed extensively against DEAE column buffer (50 mM KPO_4, pH 7.5) to remove folic acid from solution. On the following day the sample was applied to a 120 mL DEAE ion exchange column (GE Healthcare). The unbound protein fractions (containing DHFR) were collected. Remaining bound proteins and residual folic acid were eluted from the column by a linear gradient of DEAE affinity buffer supplemented with 500 mM NaCl. The column was stripped and regenerated with 1 column volume of 3 M NaCl. All fractions were analyzed by SDS-PAGE. Fractions containing highly pure (>95%) DHFR were pooled, concentrated to 1 mg/mL, flash-frozen in liquid nitrogen, and stored at −80E C.

Structure Determination and Refinement

The recombinant proteins were washed in a centricon-10 with 10 mM HEPES buffer, pH 7.4 and concentrated to 33.2 mg/mL. The protein was incubated with NADPH and an excess of the inhibitor for one hour over ice prior to crystallization using the hanging drop vapor diffusion method. The reservoir solution contained 100 mM KPO_4, pH 6.9, 60% saturated NH_4SO_4, 3% v/v ethanol. Protein droplets contained 100 mM KPO_4, pH 6.9, 30% saturated NH_4SO_4. Crystals of both mutant and wild type DHFR complexes grew over several days time at 14E C and are trigonal, space group H_3 and diffracted to 1.3 Å resolution. Data were collected at liquid N_2 temperatures on an Rigaku RaxisIV imaging plate system and then later on beamlines 11-1 and 9-2 at the Stanford Synchrotron Research Laboratory (SSRL) imaging plate system and the data processed with using Mosflm[41]. The Rmerge for all data was 0.063 with a 3-fold multiplicity. The overall completeness of the data was 94.8 and 92.8 for data in the shell between 2.05 and 2.15 Å. The data for the ternary complex refined to 17.9% for all data and 25.9% for the test data (5%) (Table 3).

The structure was solved by molecular replacement methods using the coordinates for human DHFR (u072) in the program Molref[41]. Inspection of the resulting difference electron density maps were made using the program COOT[42] running on a Mac G5 workstation revealed density for a ternary complex. The final cycles of refinement were carried out using the program Refmac5 in the CCP4 suite of programs. The Ramachandran conformational parameters from the last cycle of refinement generated by PROCHECK[43] showed that more than 91% of the residues have the most favored conformation and none are in the disallowed regions. Coordinates for these structures have been deposited with the Protein Data Bank (PDB code ???).

Supplementary Material

Refer to Web version on PubMed Central for supplementary material.

Acknowledgement

This work was supported, in part, by a grant from the National Institutes of Health and National Institute of Allergy and Infectious Diseases AI069966 (AG) and the National Institute of General medical Sciences GM51670 (VC).

Reference

1. Chan DCM, Anderson AC. Towards Species-specific Antifolates. Curr. Med. Chem 2006;13:377–398. [PubMed: 16475929]
2. Hawser S, Lociuro S, Islam K. Dihydrofolate Reductase Inhibitors as Antibacterial Agents. Biochem. Pharmacol 2006;71:941–948. [PubMed: 16359642]
3. Gmeiner HW. Novel Chemical Strategies for Thymidylate Synthase Inhibition. Curr. Med.Chem 2005;12:191–202. [PubMed: 15638735]
4. Gangjee A, Kurup S, Namjoshi O. Dihydrofolate Reductase as a Target for Chemotherapy in Parasites. Curr. Pharm. Des 2007;13:609–639. [PubMed: 17346178]
5. Berman EM, Werbel LM. The Renewed Potential for Folate Antagonists in Contemporary Cancer Chemotherapy. J. Med. Chem 1991;34:479–485. [PubMed: 1995868]
6. Blakley, RL. Dihydrofolate Reductase. In: Blakley, RL.; Benkovic, SJ., editors. Folate and Pterins. Vol. Vol. I. New York: Wiley-Interscience; 1984. p. 191-253.
7. MacKenzie, RE. Biogenesis and Interconversion of Substituted Tetrahydrofolates. In: Blakley, RL.; Benkovic, SJ., editors. Folates and Pterins Chemistry and Biochemistry. Vol. Vol. I. New York: Wiley; 1984. p. 255-306.
8. Petero GJ, Kohne CH. Fluoropyrimidines as Antifolate Drugs. Antifolate Drugs Cancer Ther 1999:101–145.
9. Rosowsky, A. Chemistry and Biological Activity of Antifolates. In: Ellis, GP.; West, GB., editors. Progress in Medicinal Chemistry. Amsterdam: Elsevier Science Publishers; 1989. p. 1-252.
10. Gangjee A, Elzein E, Kothare M, Vasudevan A. Classical and Nonclassical Antifolates as Potential Antitumor, Antipneumocystis and Antitoxoplasma Agents. Curr. Pharm. Des 1996;2:263–280.
11. Taylor EC, Kuhnt D, Shih C, Rinzel SM, Grindey GB, Barredo J, Jannatipour M, Moran RA. Dideazatetrahydrofolate Analogue Lacking a Chiral Center at C-6, *N*-[4-[2-(2-Amino-3,4-dihydro-4-oxo-*7H*-pyrrolo[2,3-*d*]pyrimidin-5-y1)ethylbenzoyl]-L glutamic Acid, Is an Inhibitor of Thymidylate Synthase. J. Med. Chem 1992;35:4450–4454. [PubMed: 1447744]
12. Jackman AL, Taylor GA, Gibson W, Kimbell R, Brown M, Calvert AH, Judson IR, Hughes LR. ICI D1694, a Quinazoline Antifolate Thymidylate Synthase Inhibitor That Is a Potent Inhibitor of L1210 Tumour Cell Growth in Vitro and in Vivo: A New Agent for Clinical Study. Cancer Res 1991;51:5579–5586. [PubMed: 1913676]
13. Bertino, JR.; Kamen, B.; Romanini, A. Folate Antagonists. In: Holland, JF.; Frei, E.; Bast, RC.; Kufe, DW.; Morton, DL.; Weichselbaum, RR., editors. Cancer Medicine. Vol. Vol. 1. Baltimore, MD: Williams and Wilkins; 1997. p. 907-921.
14. Gibson W, Bisset GMF, Marsham PR, Kelland LR, Judson IR, Jackman AL. The Measurement of Polyglutamate Metabolites of the Thymidylate Synthase Inhibitor, ICI D1694,in Mouse and Human Cultured Cells. Biochem. Pharmacol 1993;45:863–869. [PubMed: 7680860]
15. Sikora E, Jackman AL, Newell DF, Calvert AH. Formation and Retention and Biological Activity of N10-Propargyl-5,8-dideazafolic Acid (CB3717) Polyglutamates in L1210 Cells in Vitro. Biochem. Pharmacol 1988;37:4047–4054. [PubMed: 2461200]
16. Jackman AL, Newell DR, Gibson W, Jodrell DI, Taylor GA, Bishop JA, Hughes LR, Calvert AH. The Biochemical Pharmacology of the Thymidylate Synthase Inhibitor 2-Desamino-2-methyl-N10-propargyl-5,8-dideazafolic Acid (IC1 198583). Biochem. Pharmacol 1991;41:1885–1895. [PubMed: 1741766]
17. Nair MG, Abraham A, McGuire JJ, Kisliuk RL, Galivan J. Polyglutamylation as a Determinant of Cytotoxicity of Classical Folate Analogue Inhibitors of Thymidylate Synthase and Glycinamide Ribonucleotide Formyltransferase. Cell. Pharmacol 1994;1:245–249.

18. Gangjee A, Qiu Y, Li W, Kisliuk RL. Potent Dual Thymidylate Synthase and Dihydrofolate Reductase Inhibitors: Classical and Nonclassical 2-Amino-4-oxo-5-arylthio-substituted-6-methylthieno[2,3-*d*] pyrimidine Antifolates. J. Med. Chem 2008;51:5789–5797. [PubMed: 18800768]
19. We thank the Developmental Therapeutics Program of the National Cancer Institute for performing the in vitro anticancer evaluation.
20. Tripos Inc., 1699 South Handley Rd, Suite 303, St. Louis, MO 63144
21. Assaraf YG. Molecular Basis of Antifolate Resistance. Cancer Metastasis Rev 2007;26:153–181. [PubMed: 17333344]
22. Matherly LH, Hou Z. Structure and Function of the Reduced Folate Carrier a Paradigm of a Major Facilitator Superfamily Mammalian Nutrient Transporter. Vitam. Horm 2008;79:145–184. [PubMed: 18804694]
23. Cao, W.; Matherly, LH. Structural Determinants of Folate and Antifolate Membrane Transport by the Reduced Folate Carrier. In: Lash, LH., editor. Drug Metabolism and Transport. Totowa: Humana Press; 2005. p. 291-318.
24. Fry DW, Jackson RC. Membrane Transport Alterations as a Mechanism of Resistance to Anticancer Agents. Cancer SurV 1986;5:47–49. [PubMed: 3297313]
25. Schornagel JH, Pinard MF, Westerhof GR, Kathmann I, Molthoff CFM, Jolivet J, Jansen G. Functional Aspects of Membrane Folate Receptors Expressed in Human Breast Cancer Lines with Inherent and Acquired Transport-Related Resistance to Methotrexate. Proc.Am. Assoc. Cancer Res 1994;35:302.
26. Wong SC, Zhang L, Witt TL, Proefke SA, Bhushan A, Matherly LH. Impaired Membrane Transport in Methotrexate-Resistant CCRF-CEM Cells Involves Early Translation Termination and Increased Turnover of a Mutant Reduced Folate Carrier. J. Biol. Chem 1999;274:10388–10394. [PubMed: 10187828]
27. Webber SE, Bleckman TM, Attard J, Deal JG, Katherdekar V, Welsh KM, Webber S, Janson CA, Matthews DA, Smith WW, Freer ST, Jordan SR, Bacquet RJ, Howland EF, Booth CJL, Ward RW, Hermann SM, White J, Morse CA, Hilliard JA, Bartlett CA. Design of Thymidylate Synthase Inhibitors Using Protein Crystal Structures: The Synthesis and Biological Evaluation of a Novel Class of 5-Substituted Quinazolines. J. Med. Chem 1993;36:733–746. [PubMed: 8459400]
28. Hughes, A.; Calvert, AH. Preclinical and Clinical Studies with the Novel Thymidylate Synthase Inhibitor Nolatrexed Dihydrochloride (Thymitaq, AG337). In: Jackman, AL., editor. Antifolate Drugs in Cancer Therapy. Totowa: Humana Press; 1999. p. 229-241.
29. Gangjee A, Guo X, Queener SF, Cody V, Galitsky N, Luft JR, Pangborn W. Selective *Pneumocystis carinii* Dihydrofolate Reductase Inhibitors: Design, Synthesis, and Biological Evaluation of New 2,4-Diamino-5-substituted-furo[2,3-*d*]pyrimidines. J. Med. Chem 1998;41:1263–1271. [PubMed: 9548816]
30. Klon EA, Heroux A, Ross LJ, Pathak V, Johnson AC, Piper JR, Borhani WD. Atomic Structures of Human Dihydrofolate Reductase Complexed with NADPH and two Lipophilic Antifolates at 1.09 Å and 1.05 Å Resolution. J. Mol. Biol 2002;320:677–693. [PubMed: 12096917]
31. Kovacs JA, Hiemenz JW, Macher AM, Stover D, Murray HW, Shelhamer J, Lane HC, Urmacher U, Honig C, Longo DL, Parker MM, Nataneon JE, Parrillo JE, Fauci AS, Pizzo PA, Maeur H. *Pneumocystis carinii* pneumonia: a Comparison between Patients with the Acquired Immunodeficiency Syndrome and Patients with other Immunodeficiencies. Ann. Intern. Med 1984;100:68–71.
32. Klepser ME, Klepser TB. Drug Treatment of HIV-related Opportunistic Infections. Drugs 1997;53:40–73. [PubMed: 9010648]
33. Gewald K. Heterocyclen aus CH-aciden nitrilen. VII. 2-Aminothiophene aus α-oxo-Mercaptanen und Methylenaktiven Nitrilen. Chem. Ber 1966;98:3571–3577.
34. Gangjee A, Qiu Y, Kisliuk RL. Synthesis of Classical and Nonclassical 2-Amino-4-oxo-6-benzyl-thieno[2,3-d]pyrimidines as Potential Thymidylate Synthase Inhibitors. J. Heterocycl. Chem 2004;41:941–946.
35. Taylor EC, Young WB, Chaudhari R, Patel M. Synthesis of a Regioisomer of N-{4-[2-(2-amino-4 (3*H*)-oxo-7H-pyrrolo[2,3-*d*]pyrimidin-5-yl)ethyl]benzoyl}-L-glutamic Acid (LY231514), an Active Thymidylate Synthase Inhibitor and Antitumor Agent. Heterocycles 1993;36:1897–1908.

36. Itoh T, Mase T. A General Palladium-Catalyzed Coupling of Aryl Bromides/Triflates and Thiols. Org. Lett 2004;24:4587–4590. [PubMed: 15548082]

37. Gangjee A, Yu J, McGuire JJ, Cody V, Galitsky N, Kisliuk RL, Queener SF. Design, Synthesis, and X-ray Crystal Structure of a Potent Dual Inhibitor of Thymidylate Synthase and Dihyhdrofolate Reductase as an Antitumor Agent. J. Med. Chem 2003;43:3837–3851. [PubMed: 11052789]

38. Cody V, Galitsky N, Luft JR, Pangborn W, Gangjee A, Devraj R, Queener SF, Blakely RL. Comparison of Ternary Complexes of *Pneumocystis carinii* and Wild Type Human Dihydrofolate Reductase With a Novel Classical Antitumor Furo[2,3-*d*]pyrimidine Antifolate. Acta Cryst 1997;D53:638–649.

39. Kisliuk RL, Strumpf D, Gaumont Y, Leary RP, Plante L. Diastereoisomers of 5,10-Methylene-5,6,7,8-tetrahydropteroyl-D glutamic Acid. J. Med. Chem 1977;20:1531–1533. [PubMed: 410932]

40. Wahba AJ, Friedkin M. The Enzymatic Synthesis of Thymidylate. Early Steps in the Purification of Thymidylate Synthetase of *Escherichia coli*. J. Biol. Chem 1962;237:3794–3801. [PubMed: 13998281]

41. Collaborative Computational Project, Number 4, The CCP4 Suite: Programs for Protein Crystallography. Acta Crystallogr 1994;D50:760–763.

42. Emsley P, Cowtan K. Coot: Model-Building Tools for Molecular Graphics. Acta Crystallogr 2004;D60:2126–2132.

43. Laskowski RA, MacArthur MW, Moss DS, Thornton JM. PROCHECK: A Prorgram to Check the Stereochemical Quality of Protein Structures. J. Applied Crystal 1993;26:283–291.

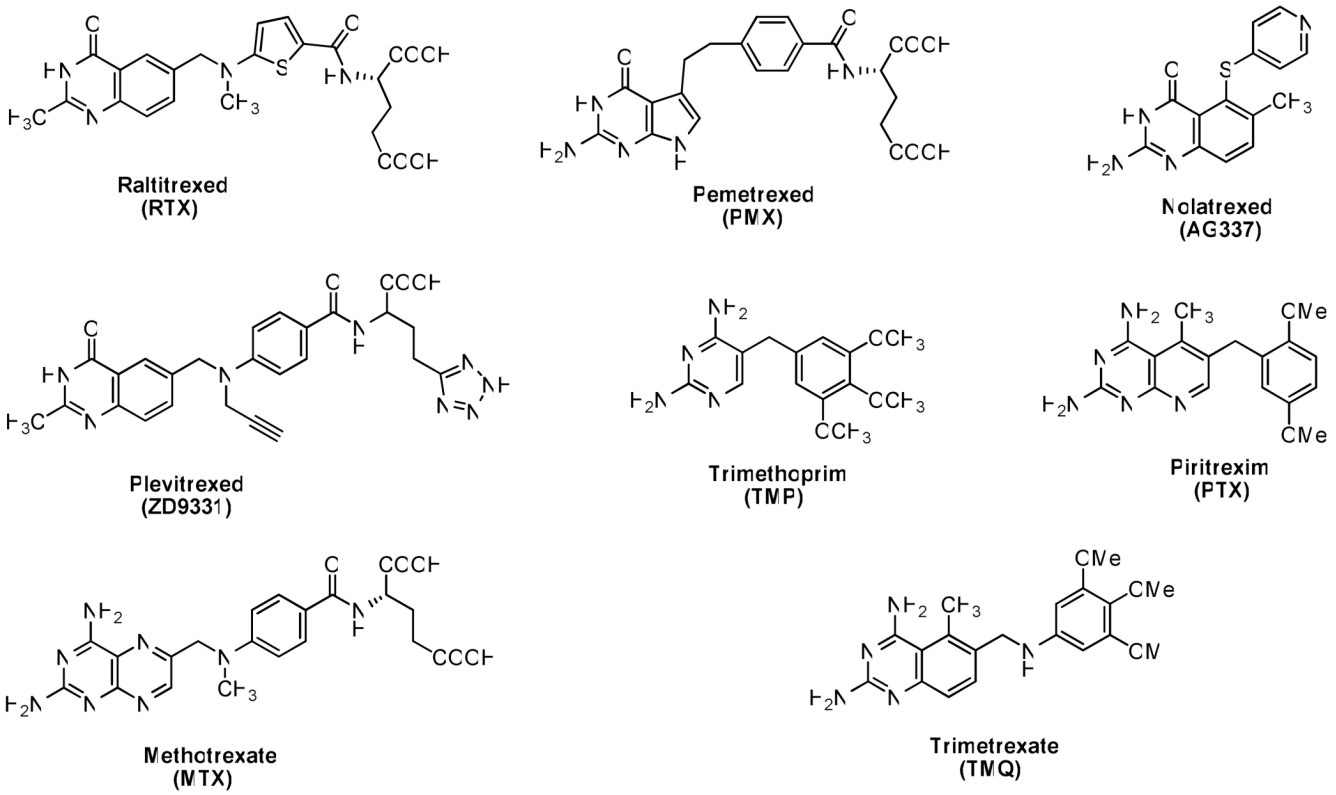

Figure 1.
Representative antifolates.

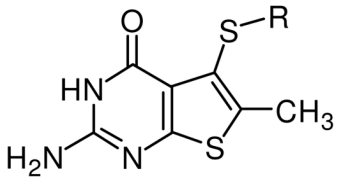

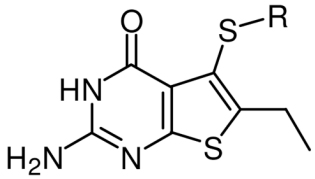

1 R = 4-C_6H_4-CO-L-Glu
1a R = Ph
1b R = 4-Cl-Ph
1c R = 4-NO_2-Ph
1d R = 2,5-di-OMe-Ph
1e R = 3,4-di-Cl-Ph
1f R = 3,5-di-Cl-Ph
1g R = 2-Naphthyl
1h R = Pyridin-4-yl
1i R = 4-F-Ph

2 R = 4-C_6H_4-CO-L-Glu
2a R = Ph
2b R = 4-Cl-Ph
2c R = 4-NO_2-Ph
2d R = 2,5-di-OMe-Ph
2e R = 3,4-di-Cl-Ph
2f R = 3,5-di-Cl-Ph
2g R = 2-Naphthyl
2h R = Pyridin-4-yl
2i R = 4-F-Ph

2j R = 4-Br-Ph
2k R = 3-Cl-Ph
2l R = 3,5-di-OMe-Ph
2m R = 2-Cl-Ph

Figure 2.
6-Methyl and Target 6-Ethyl–2-amino-4-oxo-5-substituted thieno[2,3-*d*]pyrimidines.

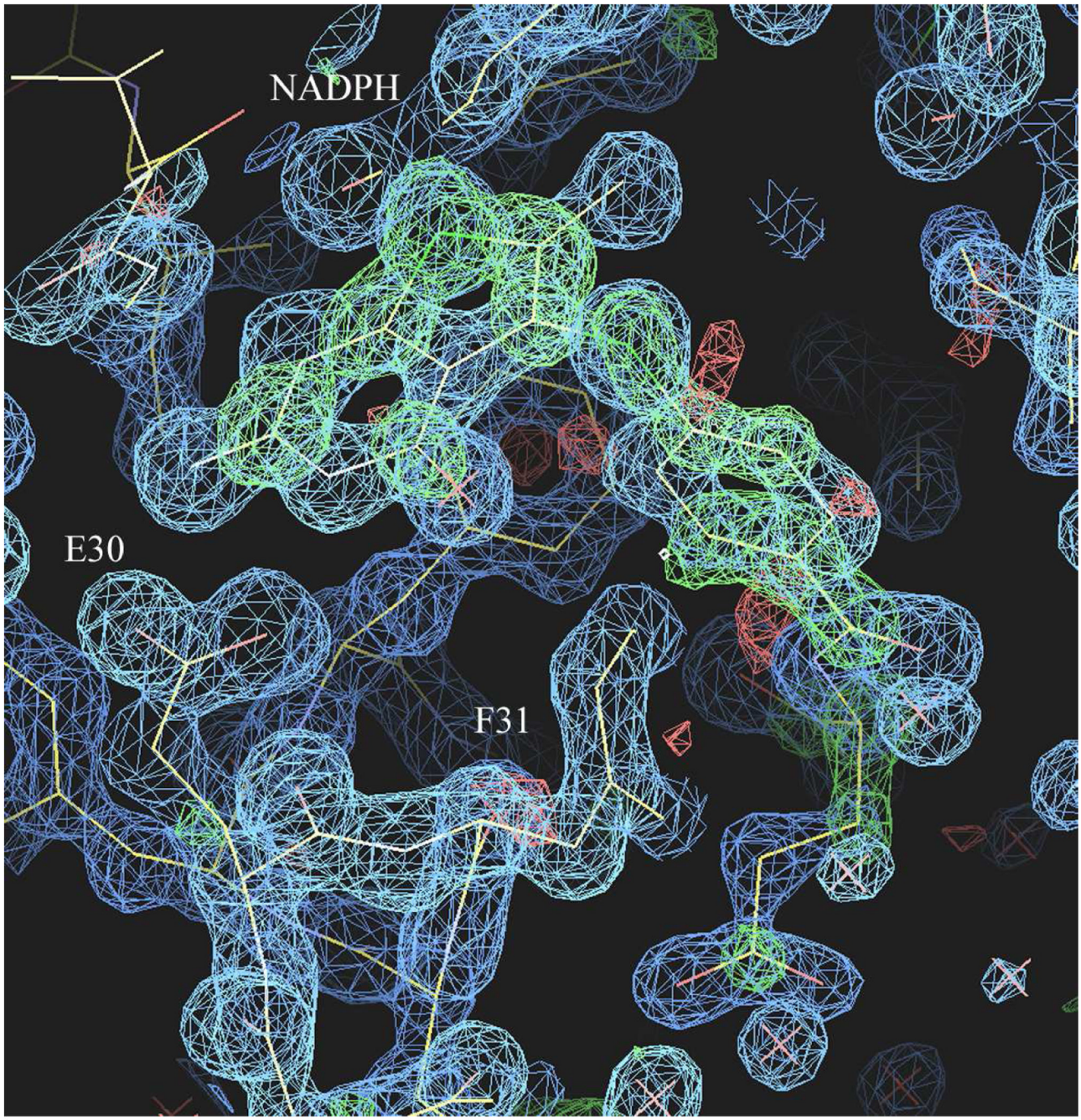

Figure 3.
Difference electron density map (2Fo-Fc, 1σ blue, Fo-Fc 3σ green) for the ternary complex of NADPH and **1** in human DHFR

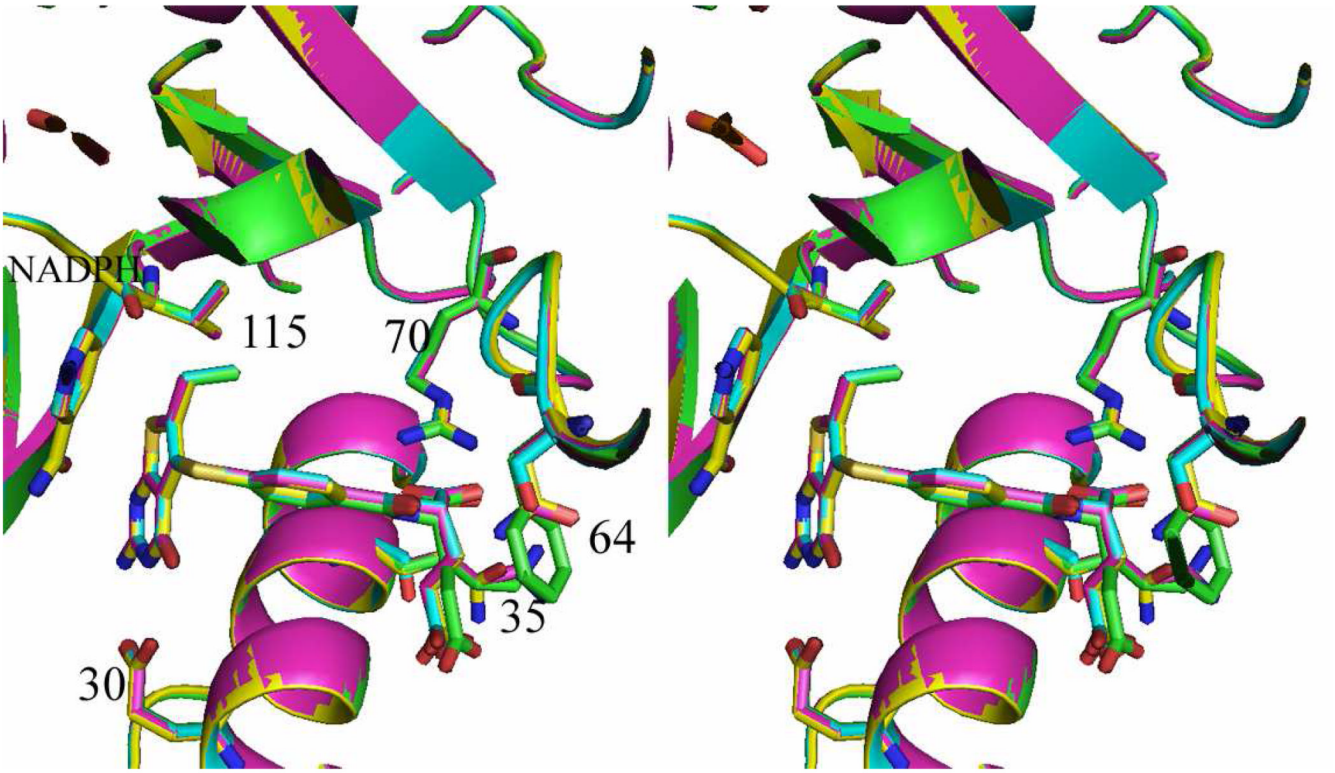

Figure 4.
Stereoview of superposition of active site for human DHFR-Q35K/N64F double mutant ternary complex with the inhibitor **2** and NADPH (green), human DHFR-Q35S/N64S double mutant ternary complex with the inhibitor **2** and NADPH (cyan), human DHFR-Q35K single mutant ternary complex with **1** (violet) and human DHFR ternary complex with **1** (yellow). The figure was prepared by PyMol.

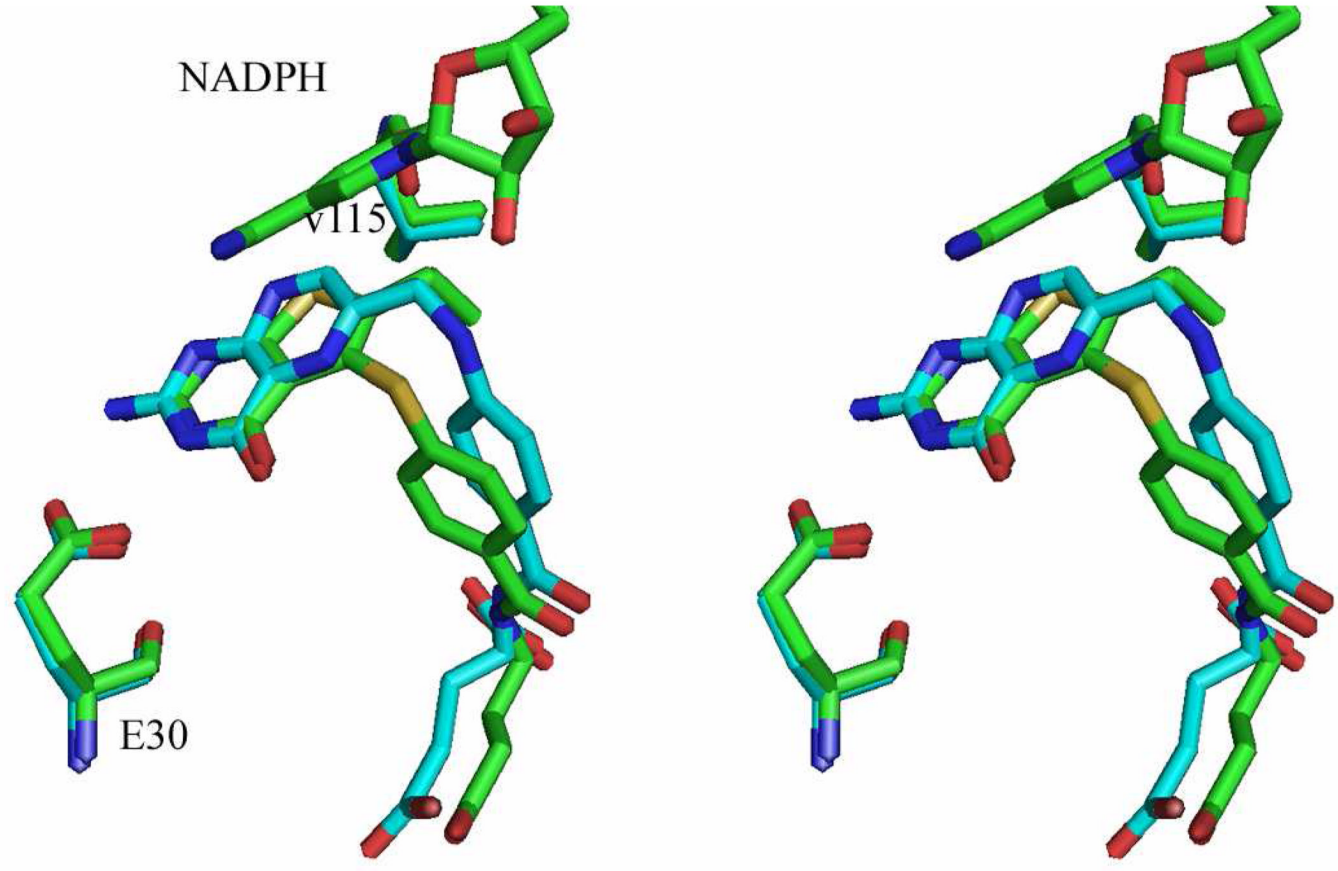

Figure 5.
Stereoview of the superposition of folate (cyan) from hDHFR (PDB1drf) on the structure of the hDHFR NADPH double mutant protein Q35K/N64F with **2** (green).

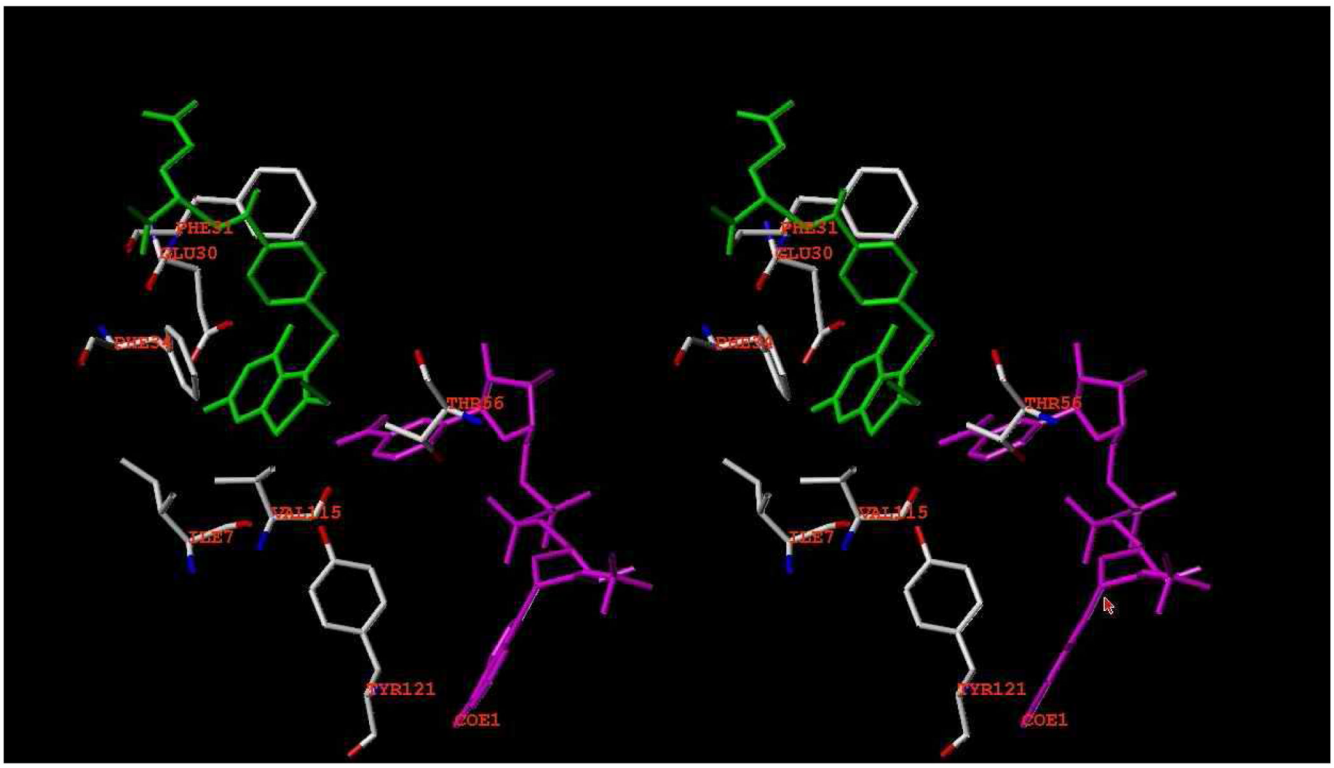

Figure 6.
Stereoview of active site for human DHFR-Q35S/N64S double mutant ternary complex with the inhibitor **2** and NADPH. The figure was prepared by SYBY 8.0.

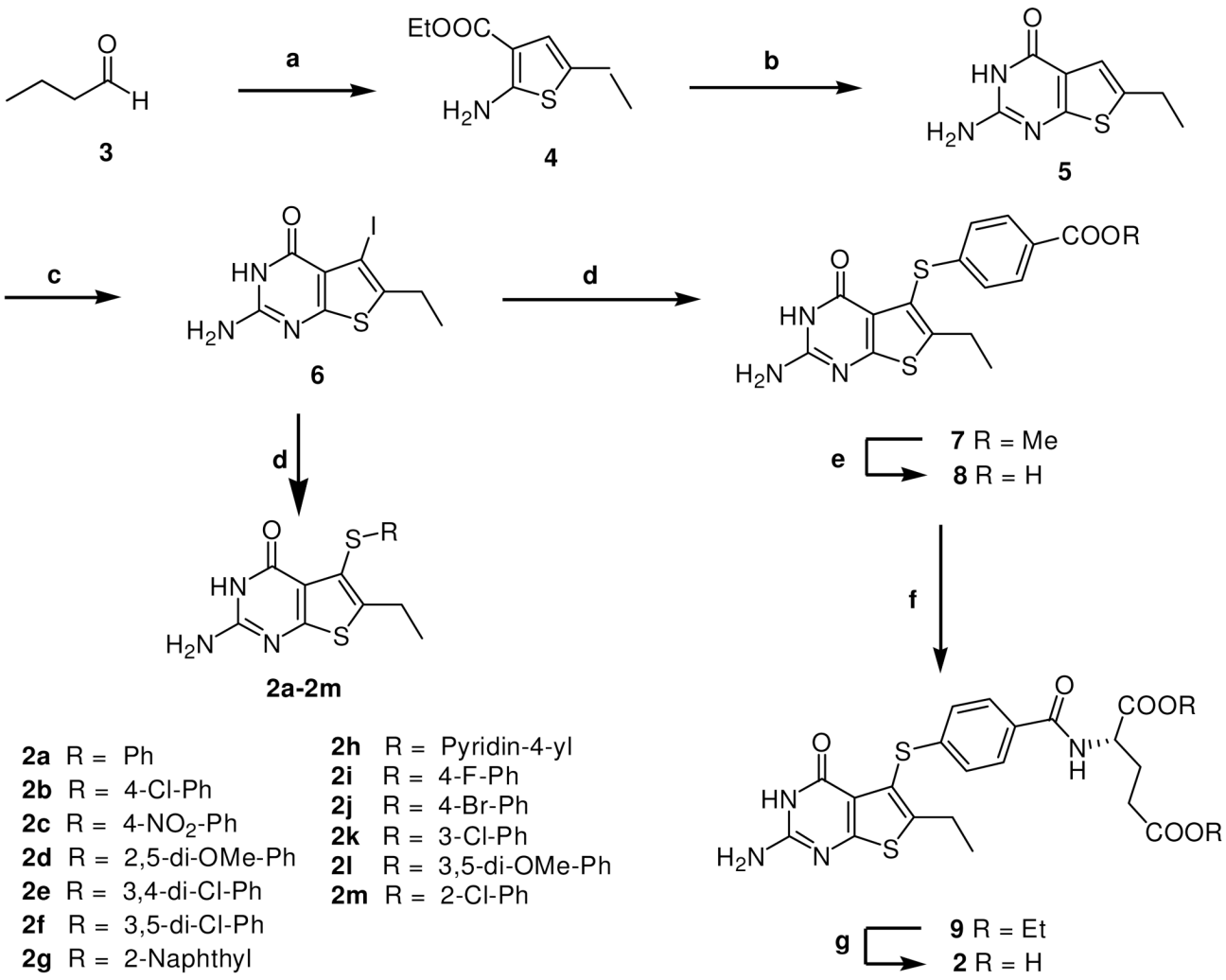

Scheme 1a.

[a] Reagents: (a) Ethylcyanoacetate, Et_3N, Sulfur, DMF, 55 °C, 3h; (b) carbamimidic chloride hydrochloride, $DMSO_2$, 120 °C, 1 h; (c) (1) $Hg(AcO)_2$, AcOH, 100 °C, 3 h; (2) I_2, CH_2Cl_2, rt, 5 h; (d) thiols, $Pd_2(dba)_3$, Xantphos, *i*-Pr_2NEt, DMF, microwave 190 °C, 30 min; (e) 1 N NaOH, MeOH; (f) Lglutamate hydrochloride, 2-chloro-4,6-dimethoxy-1,3,5-triazine, *N*-methylmorpholine, DMF, rt, 5h; (g) 1 N NaOH, EtOH.

Table 1

Inhibitory Concentrations (IC_{50} in μM) against TS and DHFR.[a]

compound	TS (μM)			DHFR (μM)			
	human[b]	*E. coli*[b]	*T. gondii*[e]	human[c]	*E. coli*[d]	*T. gondii*[e]	rh/tg[f]
1[g]	0.04	0.04	0.036	0.02	0.2	0.008	2.5
2	0.054	0.018	0.09	0.019	1.0	0.0021	9
2a	5.6	28	8.4	2.6	>33 (10)[h]	0.033	79
2b	0.75	2.5	2.2	0.3	42	0.009	33
2c	0.22	1.7	1.0	0.26	39	0.0087	30
2d	4.6	>23 (11)	>23 (29)	0.84	>28 (0)	0.014	60
2e	0.23	2.3	1.0	0.29	22	0.0081	36
2f	0.69	1.2	1.6	0.28	>2.8 (0)	0.014	20
2g	2.3	1.4	1.1	2.2	28	0.0084	262
2h	0.28	2.0	1.7	0.35	>33 (17)	0.017	21
2i	1.3	2.9	2.6	0.62	>31 (15)	0.025	25
2j	0.39	2.2	2.2	0.26	29	0.013	20
2k	0.38	2.3	1.8	0.3	>3.0 (0)	0.012	25
2l	1.2	1.8	2.3	0.54	>27 (0)	0.024	23
2m	1.1	2.0	2.5	0.6	>33 (0)	0.027	22
Pemetrexed[i]	9.5	76	2.8	6.6	230	0.43	15.35
PDDF[j]	0.085	0.019	0.43	1.9	23	0.22	8.6
MTX	nd	nd	nd	0.02	0.0088	0.033	0.6
Trimethoprim	nd	nd	nd	>340 (22)	0.01	6.8	>50

[a]The percent inhibition was determined at a minimum of four inhibitor concentrations within 20% of the 50% point. The standard deviations for determination of 50% points were within ± 10% of the value given.

[b]Kindly provided by Dr. Frank Maley, New York State Department of Health.

[c]Kindly provided by Dr. Karen Anderson, Yale University, New Haven CT.

[d]Kindly provided by Dr. J. H.Freisheim, Medical College of Ohio, Toledo, OH.

[e] Kindly provided by Dr. R. L. Blakley, St. Jude Children's hospital, Memphis TN.

[f] rh/tg is Selectivity Ratio for *T. gondii* DHFR and is the IC_{50} against rhDHFR / IC_{50} against *T. gondii* DHFR.

[g] Data derived from ref[18],nd = not determined.

[h] Numbers in parentheses indicate the % inhibition at the stated concentration.

[i] Kindly provided by Dr. Chuan Shih, Eli Lilly and Co.

[j] Kindly provided by Dr. M. G. Nair, University of South Alabama.

Table 2

Cytotoxic Evaluation (GI_{50}, M) of Compounds **1** and **2** against Selected Tumor Cell Lines.

cell line	GI_{50} of 1 (M)	GI_{50} of 2 (M)
	Leukemia	
CCRF-CEM	9.45×10^{-5}	8.53×10^{-7}
HL-60 (TB)		4.97×10^{-7}
MOLT-4	$>1.00 \times 10^{-4}$	4.78×10^{-6}
	Non-Small Cell Lung Cancer	
NCI-H460	4.12×10^{-5}	9.59×10^{-7}
NCI-H525	$>1.00 \times 10^{-4}$	7.80×10^{-6}
NCI-H23	$>1.00 \times 10^{-4}$	9.40×10^{-6}
	Colon Cancer	
HCC-2998	$>1.00 \times 10^{-4}$	9.65×10^{-7}
HCT-116	$>1.00 \times 10^{-4}$	2.84×10^{-7}
	Melanoma	
LOX IMVI	6.56×10^{-5}	9.09×10^{-8}
M14	$>1.00 \times 10^{-4}$	4.32×10^{-6}
	Ovarian Cancer	
OVCAR-8	$>1.00 \times 10^{-4}$	5.79×10^{-7}
	Renal Cancer	
786-0	$>1.00 \times 10^{-4}$	8.17×10^{-7}
SN12C	$>1.00 \times 10^{-4}$	3.31×10^{-6}

Table 3

Data collection and refinement statistics for human DHFR-NADPH-**2** ternary complexes.

Data collection	**Q35S/N64S NADPH-2**	**Q35K/N64F NADPH-2**	**Wild type NADPH-1**	**Q35K NADPH-1**
PDB accession #	3 ghc	3ghv	3ghw	3gi2
Space group	H3	H3	H3	H3
Cell dimensions (Å)	84.36 77.77	84.21 78.03	84.56 78.05	84.57 77.94
Beamline	SSRL 11-1	SSRL 11-1	SSRL 9-2	SSRL 9-2
Resolution (Å)	1.01	1.20	1.20	1.50
Wavelength (Å)	1.00	1.00	1.00	1.00
R_{sym} (%) [a,b]	0.050 (0.162)	0.058 (0.121)	0.036(2.3)	0.046 (0.29)
R_{merge}	0.045 (0.14)	0.044 (0.10)	0.114(4.2)	0.037 (0.25)
Completeness (%) [a]	99.8 (95.3)	100.0 (99.8)	100.0 (94.0)	98.9 (98.9)
Observed reflections	269,146	388,944	839,426	64,773
Unique reflections	50,745	50,446	85,159	32,939
I/σ(I)	23.0 (10.3)	26.3 (11.2)	15.1 (0.3)	11.6 (2.5)
Multiplicity [a]	5.3 (4.3)	5.3 (4.3)	9.9 (4.1)	2.0 (1.9)
Refinement and model quality				
Resolution range (Å)	26.0 – 1.30	53.3 – 1.30	22.59-1.24	42.30-1.53
No. of reflections	48155	48184	56,537	29,450
R-factor [c]	17.0	15.9	18.0	15.7
R_{free}-factor [d]	19.8	18.3	20.0	20.1
Total protein atoms	1942	2030	1933	1939
Total water atoms	354	384	347	358
Average B-factor ($Å^2$)	13.8	14.0	18.2	18.3
Rms deviation from ideal				
Bond lengths (Å)	0.009	0.029	0.009	0.010
Bond angles (°)	1.858	1.943	1.76	1.73
Luzzati	0.131	0.127	0.144	0.143
Ramachandran plot				
Most favored regions (%)	97.8	98.9	98.9	97.8
Additional allowed regions (%)	2.2	1.1	1.1	2.2
Generously allowed regions (%)	0.0	0.0	0.0	0.0
Disallowed regions (%)	0.0	0.0	0.0	0.0

[a] The values in parentheses refer to data in the highest resolution shell.

[b] $R_{sym} = \sum h \sum i |I_{h,i} - \langle I_h \rangle| / \sum h \sum i |I_{h,i}|$, where $\langle I_h \rangle$ is the mean intensity of a set of equivalent reflections.

[c] R-factor $= \sum |F_{obs} - F_{calc}| / \sum F_{obs}$, where F_{obs} and F_{calc} are observed and calculated structure factor amplitudes.

[d] R_{free}-factor was calculated for R-factor for a random 5% subset of all reflections.